Impossible Trinity in Underwater Optical Wireless Communication

Qiwei Wang*†, Chi Lin*†, Yi Wang*†, Yu Sun*†, Lei Wang*†, Xin Fan*†, Guowei Wu*†
*School of Software Technology & DUT-RU International School of Information Science and Engineering, Dalian University of Technology, Dalian 116024, China
†Key Laboratory for Ubiquitous Network and Service Software of Liaoning Province, Dalian 116621, China
Email: q.wang@mail.dlut.edu.cn, c.lin@dlut.edu.cn, dlutwangyi@dlut.edu.cn, yusun.dut@gmail.com, lei.wang@ieee.org, xin.fan@dlut.edu.cn, wgwdut@dlut.edu.cn

***Abstract*—Underwater Optical Wireless Communication (UOWC) is considered a promising approach, offering the potential for flexible and high-speed communication under the surface of the water. However, the interdependent relationship among three key performance elements, namely communication distance, bit error rate, and communication rate, has been largely overlooked. This oversight impedes the complete utilization of the system performance. In this work, we innovatively introduce a "UOWC Impossible Trinity" model and theorems to establish relationships among the three key performance elements, which clarify the inherent constraints within UOWC system optimization. Moreover, we formulate the Underwater Optical Communication Trade-offs (UOCT) Problem to maximize communication performance. Furthermore, we provide feasible non-dominated solution sets, considering the constraints of real environments and user demands of specific scenarios. Our model has been validated by extensive simulations, demonstrating that our approach not only clarifies fundamental limitations of UOWC systems, but also provides practical guidelines for designing and optimizing the systems. Our approach has been experimentally validated with an impressive accuracy of over 95%, surpassing conventional models, which not only enhances the understanding of UOWC system optimization but also validates the existence of inherent trade-offs. Furthermore, our approach demonstrates a significant increase in communication distance, outperforming traditional methods by more than 20%.**

I. Introduction

Underwater Optical Wireless Communication (UOWC) is a cutting-edge technology that utilizes visible light to transmit data in underwater environments [1], [2]. As an emerging domain, UOWC is garnering significant attention and is the subject of extensive research due to its numerous advantages, including high bandwidth, low latency, energy efficiency, minimal pollution, and compact equipment requirements [3], [4]. This technology holds the potential for transformative advancements in underwater communication. The flexibility and efficiency of UOWC open up vast possibilities for applications in various domains, such as naval military operations, ocean exploration, marine environmental monitoring, marine engineering, and underwater robotics [5].

In the realm of UOWC systems, achieving efficient, reliable, and long-range communication is paramount [6]. These intertwined requirements exert a significant influence on the quality of communication. In reality, due to the inherent characteristics and constraints of these systems, these goals often appear to be contradictory. Current technological innovations and optimization strategies often lack a holistic balance among these key performance parameters. They may target one or two aspects and overlook others in the process. This oversight can lead to the waste of precious energy resources or the inability to optimally utilize performance capabilities according to the actual communication scenario. Consequently, the overall communication efficiency of UOWC can be severely impaired, undermining its robustness and usability, and thus forfeiting many potential application scenarios.

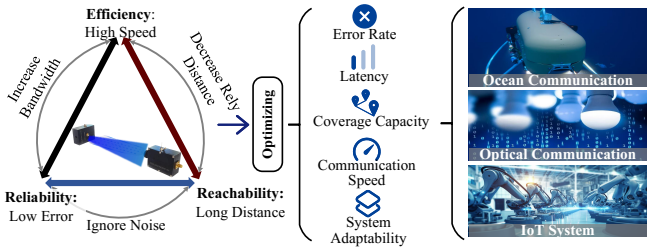

Fig. 1. Impossible Trinity and its Applications

The main objectives of this research are as follows: (i) We aim to optimize multiple performance elements within the UOWC system, by establishing explicit relationships and formulating precise models despite their complex and undefined connections. (ii) We attempt to enhance performance within the constraints of environmental dynamics and system fluctuations, finding the boundary of performance improvements and seeking simultaneous enhancement of multiple performance metrics. (iii) We try to tackle the NP-hardness of the multi-objective optimization problem by providing reasonable and feasible solutions within practical time constraints.

Technically, we encountered the following challenges:

- Within the UOWC system framework, multiple performance elements require optimization. The connections among these elements are complex and undefined, with multiple parameters that impact each other, making the challenge. It is non-trivial to establish explicit relations among these elements and formulate precise models.
- In the process of model optimization, performance improvement is not unbounded. In addition to the per-

Corresponding author: **Chi Lin***† (E-mail: c.lin@dlut.edu.cn).

979-8-3503-5171-2/24/$31.00 ©2024 IEEE

formance constraints among the elements, optimization must consider environmental dynamic interferences and system performance fluctuations, making it difficult to seek directions and space for simultaneous enhancement of multiple performance metrics.
- The issue of multi-objective optimization in the context of complex nonlinear relationships corresponds to NP-hard problems. Providing reasonable and feasible solutions within a political time poses considerable challenges.

To address these challenges and achieve our goals, we first establish the "**UOWC Impossible Trinity**" model based on UOWC fundamental communication principles, channel models, and practical scenarios, and conduct qualitative analysis on various parameters and indicators. Then the "**UOWC Impossible Trinity**" theorems are proposed based on the model to exploit its features. Finally, the accuracy of the model and the theorems are verified through simulation experiments and test-bed experiments. The contributions of this paper can be summarized as below:

- We propose a "UOWC Impossible Trinity" model, clarifying the intrinsic relationships among the three key performance elements in UOWC systems: *BER*, C, and D. This model, combined with the UOWC Impossible Trinity" theorems, provides essential insights for optimizing UOWC system performance and can be extended to other communication fields, as depicted in Fig. 1.
- We present feasible non-dominated solution sets based on the model and theorems, considering real-world environmental limitations, user-specific scenario demands, and available resources, offering valuable guidance for optimizing optical communication systems.
- We validate the model's accuracy, feasibility, superiority, and universality of the "UOWC Impossible Trinity" model through extensive simulation and test-bed experiments, demonstrating an average accuracy of over 95% and a substantial improvement of more than 20% in communication distance compared to traditional approaches.

This paper is structured as follows: Section II outlines the models and problem statement. Section III proposes the "Impossible Trinity" model and its solver. Theoretical analysis is detailed in Section IV, followed by simulations and test-bed experiments that demonstrate performance in Sections V and VI, respectively. A review of related literature is presented in Section VII. The paper is concluded in Section VIII.

II. Model and Problem Statement

In this section, we present related models and problem statement of this research.

A. System Model

The UOWC system consists of several key components, including a transmitter (Tx) and a receiver (Rx) with optical transceiver modules, signal processing units, and a power supply. The optical transceiver modules employ different modulation techniques (e.g., on-off keying (OOK), and Pulse Amplitude Modulation (PAM)) to encode and decode data onto the optical carrier.

The encoded optical signal is emitted from Tx and propagates through the water channel. During the transmission, the signal undergoes losses, and then interference impairs communication distance and accuracy. Finally, the signal reaches Rx, where it is decoded to retrieve the original information, thus accomplishing the communication.

B. Communication Distance Model

In a UOWC system, the communication distance is limited by the path loss *PL*, which is determined by attenuation loss PL_{AL} and geometrical loss PL_{GL} [7].

$$PL(D) = PL_{\mathrm{AL}}(D) + PL_{\mathrm{GL}}(D). \tag{1}$$

The attenuation loss can be quantified via the Beer-Lambert formula [8], which relates to the extinction coefficient,

$$PL_{\mathrm{AL}}(D) = 10\log_{10}\left(\mathrm{e}^{-kD}\right). \tag{2}$$

According to Haltran's model [9], the extinction coefficient k of attenuation loss can be expressed as $k = a + s$, where a and s represent absorption coefficient and the scattering coefficient, respectively. D represents the link distance between the Tx and Rx. This function is based on two implicit premises. Firstly, it assumes perfect alignment between Tx and Rx. Secondly, it assumes all scattered photons are lost, ignoring the fact that in reality, some scattered photons can still reach the receiver even after undergoing multiple scattering events.

Geometrical loss occurs during the propagation of the transmitted beam from Tx to Rx. Typically, the spreading light beam's size exceeds the receiving aperture dimensions, resulting in overfill energy loss. Therefore, diffused and semi-collimated light sources (i.e., LEDs and diffused LDs) demonstrate a significant effect on geometric divergence loss. Based on the consideration of line-of-sight (LOS) configuration and the characteristic of semi-collimated laser source with a Gaussian beamshape, geometrical loss can be approximated by

$$PL_{\mathrm{GL}}(D) \approx 10\log_{10}\left(\left(\frac{r}{\theta_{1/\mathrm{e}}D}\right)^2\right). \tag{3}$$

Here, r denotes the receiver aperture diameter and $\theta_{1/\mathrm{e}}$ refers to the full width transmitter beam divergence angle.

Therefore, Equation (1) can be represented by

$$\begin{aligned} PL(D) &= PL_{\mathrm{AL}}(D) + PL_{\mathrm{GL}}(D) \\ &\approx 10\log_{10}\left(\left(\frac{r}{\theta_{1/\mathrm{e}}D}\right)^2 \mathrm{e}^{-kD}\right). \end{aligned} \tag{4}$$

In practical scenarios, the Rx detector can capture rays that undergo multiple scattering, contrary to the assumption that the scattered rays are considered lost. To incorporate the influence of scattered rays, we present a modified rendition of Equation (4) as follows:

$$PL(D) \approx 10\log_{10}\left(\left(\frac{r}{\theta_{1/\mathrm{e}}D}\right)^2 \mathrm{e}^{-kD\left(\frac{r}{\theta_{1/\mathrm{e}}D}\right)^T}\right). \tag{5}$$

To account for the geometrical propagation of the light source, an additional term is incorporated in the negative

exponential. Equation (5) introduces the correction coefficient T, which can be determined by fitting the simulation data.

Let l denote the optical path loss measured on a linear scale (i.e., optical channel coefficient). According to the Equation (5), l can be written as

$$l \approx \left(\frac{r}{\theta_{1/e} D}\right)^2 e^{-kD\left(\frac{r}{\theta_{1/e} D}\right)^T}. \tag{6}$$

Based on Equation (6), we figure out D by multiplying $(\frac{r}{\theta_{1/e}})$ and powering $(\frac{T-1}{2})$, then multiplying $(T-1)(k\frac{r^T}{2\theta^T_{1/e}})$:

$$\begin{aligned}(1-T)\left(\frac{k}{2}\frac{r^T}{\theta^T_{1/e}}\right) D^{(1-T)} e^{(1-T)\left(\frac{k}{2}\frac{r^T}{\theta^T_{1/e}}\right) D^{(1-T)}} \\ = (1-T)\left(\frac{k}{2}\frac{r^T}{\theta^T_{1/e}}\right)\left(\frac{l\theta^2_{1/e}}{r^2}\right)^{\left(\frac{T-1}{2}\right)}.\end{aligned} \tag{7}$$

Then, we involve the real part of Lambart-W function i.e., $\mathrm{W} = (xe^x)$ [10], and D can be computed by

$$D = \left[\frac{\mathrm{W}\left(\frac{k}{2}(1-T)\left(\frac{r}{\theta_{1/e}}\right) l^{\left(\frac{T-1}{2}\right)}\right)}{\frac{k}{2}(1-T)\left(\frac{r}{\theta_{1/e}}\right)^T}\right]^{\frac{1}{1-T}}. \tag{8}$$

Besides, according to the extinction coefficient mentioned above and the hardware specifications, the received power at Rx from Tx is modeled in [11] as follows:

$$P_r = P_t \varrho_t \varrho_r \mathrm{e}^{\frac{-cD}{\cos\theta_i}} \frac{r\cos\theta_i}{2\pi D^2\left(1-\cos\theta_{1/\mathrm{e}}\right)}, \tag{9}$$

where P_r and P_t are the receive power and transmit power of Rx and Tx, ϱ_t and ϱ_r are the Tx and Rx optical efficiency respectively, and θ_i is the angle between trajectory of the Tx and Rx. Based on Equation (9), the distance D is given as:

$$D = \frac{2}{k}\mathrm{W}_0\left(\frac{k}{2}\sqrt{\frac{P_t \varrho_t \varrho_r r\cos\theta_i}{P_r 2\pi\left(1-\cos\theta_{1/\mathrm{e}}\right)}}\right) + n, \tag{10}$$

where W_0 is the real part of Lambart-W function and n is the ranging estimation noise modeled as zero mean Gaussian random variable $n \sim N\left(0, \sigma^2\right)$ with variance σ^2 [12].

C. Bit Error Rate Model

BER, in a real Additive White Gaussian Noise (AWGN) channel with single-carrier modulation such as On-Off keying (OOK), Pulse Amplitude Modulation (PAM), and Intensity Modulation (IM) * [7], [10], can be represented by signal-to-noise ratio (*SNR*) as:

$$\mathit{BER} = Q\left(\sqrt{\frac{\mathit{SNR}}{2}}\right), \tag{11}$$

where *SNR* is defined as

$$\mathit{SNR} = \frac{(\varrho_t \varrho_r)^2 v^2 l^2 P_{\mathrm{t}}}{\sigma_n^2}. \tag{12}$$

*The multi-carrier modulation technique, such as Orthogonal Frequency-Division Multiplexing (OFDM), features independent modulation of each subcarrier, each subjected to unique channel conditions. The overall *SNR* of the system is calculated by averaging the *SNR* of all subcarriers.

In Equation (12), v is the photodetector responsivity and σ_n^2 is the noise variance. The l value, in Equation (12), can be obtained from (11) and (12) which can achieve the *BER*.

$Q(z)$ is the Q-function, sometimes referred to as the Gaussian integral [13]. It is defined as

$$Q(z) = \int_z^\infty \frac{1}{\sqrt{2\pi}} e^{-u^2} du. \tag{13}$$

Note that $Q(z)$ is a monotonically decreasing function of z. Therefore, the power efficiency of a modulation scheme is defined simply as the required *SNR* for a certain bit error probability on an AWGN channel.

Based on Equation (11) and Equation (12), by replacing the result in Equation (8), we can have D by inputing *BER* as:

$$D = \left[\frac{\mathrm{W}\left(\frac{k(1-T)r}{2\theta_{1/e}}\left(\sqrt{\frac{2\sigma_n^2}{r^2(\varrho_t\varrho_r)^2 P_t}} Q^{-1}\left(\mathit{BER}\right)\right)^{\left(\frac{T-1}{2}\right)}\right)}{\frac{k(1-T)}{2}\left(\frac{r}{\theta_{1/e}}\right)^T}\right]^{\frac{1}{1-T}}. \tag{14}$$

D. Communication Speed Model

According to Shannon's Information Capacity Theorem [14], the channel's information capacity C can be achieved over the communication channel without error, based on its bandwidth in hertz and the *SNR*. C is calculated as:

$$C = B\log_2(1+\mathit{SNR}), \tag{15}$$

where B is the channel bandwidth.

E. Problem Formulation

The objective of this study is to optimize communication performance in a specific system. In UOWC, key performance indicators include communication speed, communication distance, and bit error rate, which are crucial for assessing system performance. However, these parameters are interconnected within the specific underwater environment and equipment setup, meaning that optimizing one or more parameters may impact other parameters. Hence, a comprehensive approach is needed to balance these interconnected factors and achieve an efficient and reliable UOWC system.

The problem is: *How can resources be efficiently balanced within the constraints of inherent system performance limits and practical considerations, in order to maximize system performance under specific circumstances?* Therefore, we formulate the Underwater Optical Communication Trade-offs (UOCT) Problem as follows.

UOCT Problem Definition: Letting C, D, and *BER* as the communication rate, communication distance, and average bit error rate with respect to *SNR* respectively in the system. F is denoted as the objective function, and the UOCT Problem can be formulated as:

$$\begin{aligned} &\max F = C, D, (1-\mathit{BER}) \\ s.t. \quad &C_{\text{limit}} \le C \le C_{\text{work}}, \\ &D_{\text{limit}} \le D \le D_{\text{work}}, \\ &\mathit{BER}_{\text{limit}} \ge \mathit{BER} \ge \mathit{BER}_{\text{work}}. \end{aligned} \tag{16}$$

Here, C, D, and $(1-BER)$ have a minimum threshold for system operation. These thresholds are defined as C_{limit}, D_{limit}, and $(1-BER_{\text{limit}})$, respectively. Note that *BER* is the parameter we aim to minimize. Therefore, we use $(1-BER_{\text{limit}})$ to represent the worst-case scenario. Similarly, each of these three elements carries an acceptable upper limit, exceeding which could potentially jeopardize the operational parameters of the other two elements. These upper bound limits are denoted as C_{work}, D_{work}, and $(1-BER_{\text{work}})$. The $(1-BER_{\text{work}})$ indicates the highest accuracy, which is the upper bound. And the parameters C_{work}, D_{work}, and BER_{work} satisfy:

$$\begin{aligned} C_{\text{work}} &= \max\{C \mid D \le D_{\text{work}}, (1-BER) \le (1-BER_{\text{work}})\}, \\ D_{\text{work}} &= \max\{D \mid C \le C_{\text{work}}, (1-BER) \le (1-BER_{\text{work}})\}, \\ BER_{\text{work}} &= \min\{BER \mid D \le D_{\text{work}}, C \le C_{\text{work}}\}. \end{aligned} \tag{17}$$

The issues raised in this model are both complex and challenging to resolve for several reasons: (i) the unpredictable and dynamic nature of the UOWC environment is a major factor contributing to the difficulty. Underwater conditions are influenced by various factors such as water quality, depth, temperature, salinity, and organic matter, leading to varying conditions for light propagation. (ii) The system modeling itself is intricate, as it involves numerous parameters that may not always align with the ideal assumptions made during the design phase. (iii) Achieving optimal performance in terms of communication distance, speed, and accuracy while managing constraints such as system costs, size, and environmental noise adds another layer of difficulty. Balancing these interconnected factors essential for UOWC requires careful consideration and trade-offs to arrive at an efficient and reliable UOWC system.

III. Proposed Scheme

A. Impossible Trinity Model

In UOWC system, there exists a fundamental inherent trade-off among performance elements namely communication efficiency, communication reliability, and communication distance. The inherent contradiction among the performance indicators in UOWC systems presents a challenge in achieving a balanced and coordinated scheduling. The inherent relationships of the performance elements are discussed below:

Based on Equation (11), *SNR* can be expressed as:

$$SNR = 2\left(Q^{-1}(BER)\right)^2. \tag{18}$$

According to Equation (15), *SNR* can be represented as:

$$SNR = 2^{(\frac{C}{B})} - 1. \tag{19}$$

Based on Equation (10) and (12), we have:

$$SNR = \frac{P_r 2\pi\left(1-\cos\theta_{1/e}\right)(\varrho_t\varrho_r)v^2l^2\left[\frac{2}{k}\mathrm{W}_0^{-1}\left(\frac{k}{2}D-n\right)\right]^2}{\sigma_i^2 r\cos\theta_i}. \tag{20}$$

Note that the monotonicity of this function varies with D, hence, we need to calculate its partial derivative with respect to D and analyze the sign of the partial derivative. Obtaining the partial derivative depends on the other parameters. Nevertheless, we assume that all other parameters are fixed, as $W_0^{-1}(\cdot)$ is monotonically increasing throughout its defined range, this function should also be monotonically increasing (the derivative is detailed in Section (III-B).

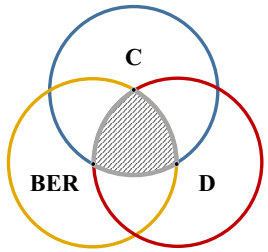

Fig. 2. Acceptable Range

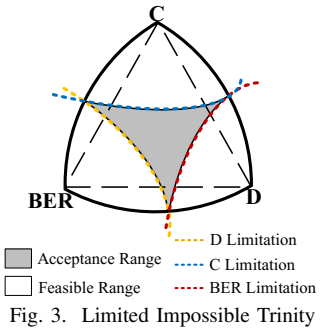

Fig. 3. Limited Impossible Trinity

As depicted in Fig. 2, each element of *BER*, C, and D exhibits a distinct range of achievable performance, which corresponds to a specific required *SNR* range. These relationships are represented by closed graphs. In practice, the required *SNR* ranges for the three elements often overlap, indicating communication feasibility. The edges of these graphs indicate the maximum values attainable for their respective elements. The distance from the center to the designated point indicates the corresponding value in the situation. This overlapping closed graph consistently features three intersection points and edges, called the **"Impossible Trinity"**.

B. Edge Curves of the Impossible Trinity

To describe the edge curves of the Impossible Trinity, we take the derivatives of *BER*, C, and D respectively. The derivatives are the curvatures of the edge curves which reflect the trend of *SNR* about the three elements.

1) Bit Error Rate (BER): The Q-function [13], namely the error function, is defined as:

$$Q(z) = \frac{1}{\sqrt{2\pi}}\int_z^\infty e^{-\frac{t^2}{2}}dt, \tag{21}$$

and its derivative is:

$$Q'(z) = -\frac{1}{\sqrt{2\pi}}e^{-\frac{z^2}{2}}. \tag{22}$$

The function $Q^{-1}(z)$ (the inverse of the Q-function) is non-trivial to differentiate, particularly because it involves a Gaussian distribution's cumulative distribution function. However, it is still possible to derive an expression for the derivative.

The derivative of $Q^{-1}(z)$ at a point z is given by the reciprocal of $Q'(z)$. Hence,

$$(Q^{-1}(z))' = \frac{1}{Q'(z)} = -\sqrt{2\pi}e^{\frac{z^2}{2}}. \tag{23}$$

Then, by taking the derivative of *SNR* with respect to *BER* in Equation (18), we obtain:

$$\begin{aligned} \frac{\mathrm{d}SNR}{\mathrm{d}BER} &= 4Q^{-1}(BER)(Q^{-1})'(BER), \\ &= -4\sqrt{2\pi}Q^{-1}(BER)e^{\frac{BER^2}{2}}. \end{aligned} \tag{24}$$

Here, we further take the second derivative based on Equation (37). We treat the function as $f(BER)\cdot g(BER)$, where

$f(BER) = -4\sqrt{2\pi}Q^{-1}(BER)$ and $g(BER) = e^{\frac{BER^2}{2}}$.

Using the product rule of differentiation, we find $f'(BER)$ and $g'(BER)$:

$$f'(BER) = -4\sqrt{2\pi}(\sqrt{2\pi}e^{\frac{BER^2}{2}}) = -8\pi e^{\frac{BER^2}{2}}, \quad (25)$$

$$g'(BER) = BERe^{\frac{BER^2}{2}}. \quad (26)$$

Substituting these results into the product rule gives the derivative of the function:

$$\begin{aligned}\frac{\mathrm{d}f(BER)}{dBER} &= (f \cdot g)'(BER) \\ &= f'(BER) \cdot g(BER) + f(BER) \cdot g'(BER), \\ &= -8\pi e^{BER^2} - 4BER\sqrt{2\pi}Q^{-1}(BER)e^{\frac{BER^2}{2}}.\end{aligned} \quad (27)$$

This expression represents the slope of changing rate of *SNR* with respect to *BER*.

2) Maximum Communication Rate (C): To differentiate the equation $SNR = 2^{(\frac{C}{B})} - 1$ with respect to C, we first use the calculus chain rule. The chain rule states that the derivative of a composed function is the derivative of the outer function times the derivative of the inner function. First, let $u = \frac{C}{B}$. Hence, $SNR = 2^u - 1$. Now, the derivative of the equation with respect to u is

$$\frac{\mathrm{d}SNR}{\mathrm{d}u} = 2^u \ln 2. \quad (28)$$

Then, the $\frac{\mathrm{d}u}{\mathrm{d}C}$ is

$$u = \frac{C}{B} \Rightarrow \frac{\mathrm{d}u}{\mathrm{d}C} = \frac{1}{B}. \quad (29)$$

The bandwidth of a channel is often a fixed characteristic, determined by the physical properties of the channel and the technology used. In many practical communication systems, the bandwidth of the channel is determined by regulatory, physical, or technological constraints. For each system, there is a constant bandwidth B influences the C.

To observe the relationship of *SNR* with respect to C, we use the derivative based on the chain rule, which is:

$$\frac{\mathrm{d}SNR}{\mathrm{d}C} = \frac{\mathrm{d}SNR}{\mathrm{d}u} \cdot \frac{\mathrm{d}u}{\mathrm{d}C} = 2^u \ln 2 \cdot \frac{1}{B} = \frac{2^{(\frac{C}{B})} \ln 2}{B}. \quad (30)$$

To find $f''(C)$, we use the rule that the derivative of $a^{g(C)}$ is $a^{g(C)} \ln(a) \cdot g'(C)$, we find:

$$\frac{\mathrm{d}}{\mathrm{d}C}\left(\frac{2^{(\frac{C}{B})} \ln 2}{B}\right) = \frac{\ln 2}{B} \cdot 2^{(\frac{C}{B})} \ln 2 \cdot \frac{1}{B} = \frac{(\ln 2)^2}{B^2} \cdot 2^{(\frac{C}{B})}. \quad (31)$$

Finally, the second derivative of *SNR* with respect to C is:

$$\frac{\mathrm{d}^2SNR}{\mathrm{d}C^2} = \frac{(\ln 2)^2}{B^2} \cdot 2^{(\frac{C}{B})}. \quad (32)$$

This expression represents the slope of changing rate of *SNR* with respect to the communication speed *C*. It is worth mentioning that the computation assumes that *B* is a constant when differentiating with respect to *C*.

3) Communication Distance (D): To differentiate the equation with respect to D, we apply the chain rule and the power rule for derivatives. Given Equation (20), we define

$$u = \frac{2}{k}\mathrm{W}_0^{-1}\left(\frac{k}{2}D - n\right). \quad (33)$$

Then, Equation (20) becomes

$$SNR = \frac{P_r 2\pi \left(1 - \cos\theta_{1/e}\right)(\varrho_t \varrho_r)u^2}{\sigma_i^2 r \cos\theta_i}. \quad (34)$$

After differentiating this equation with respect to u (using the power rule), then we have

$$\frac{\mathrm{d}SNR}{\mathrm{d}u} = 2u\frac{P_r 2\pi \left(1 - \cos\theta_{1/e}\right)(\varrho_t \varrho_r)}{\sigma_i^2 r \cos\theta_i}. \quad (35)$$

To find $\frac{\mathrm{d}u}{\mathrm{d}D}$, we differentiate u with respect to D, and we get

$$\frac{\mathrm{d}u}{\mathrm{d}D} = \left(\frac{k}{2}D - n\right)e^{\frac{k}{2}D - n}. \quad (36)$$

Afterwards, we calculate the derivative of *SNR* with respect to D by using the chain rule:

$$\begin{aligned}\frac{\mathrm{d}SNR}{\mathrm{d}D} &= \frac{\mathrm{d}SNR}{\mathrm{d}u} \cdot \frac{\mathrm{d}u}{\mathrm{d}D} \\ &= 2u\left(\frac{k}{2}D - n\right)e^{\frac{k}{2}D - n} \cdot \frac{P_r 2\pi \left(1 - \cos\theta_{1/e}\right)(\varrho_t \varrho_r)}{\sigma_i^2 r \cos\theta_i}.\end{aligned} \quad (37)$$

Then, we find the second derivative of *SNR* with respect to *D* using the chain rule. We treat the first derivative as a function of the form $f(D) = h(D) \cdot u$, where $h(D) = 2\left(\frac{k}{2}D - n\right)e^{\frac{k}{2}D - n} \cdot \frac{P_r 2\pi\left(1 - \cos\theta_{1/e}\right)(\varrho_t \varrho_r)}{\sigma_i^2 r \cos\theta_i}$, and $u = \frac{2}{k}\mathrm{W}_0^{-1}\left(\frac{k}{2}D - n\right)$.

Omit the simplification step, we finally have:

$$\begin{aligned}\frac{df}{dD} =& 2^3 \cdot e^{2(\frac{k}{2}D - n)} \cdot \left(\frac{k}{2}D - n\right)^2 \\ &\cdot \left[\frac{P_r \cdot 2\pi \cdot (1 - \cos\theta_{1/e}) \cdot (\varrho_t \varrho_r)}{k \cdot \sigma_i^2 \cdot r \cdot \cos\theta_i}\right] \\ &+ \left[\frac{k}{2} \cdot D - n + 1\right]\left[\frac{P_r \cdot 2\pi(1 - \cos\theta_{1/e}) \cdot (\varrho_t \varrho_r)}{\sigma_i^2 \cdot r \cdot \cos\theta_i}\right].\end{aligned} \quad (38)$$

Based on Equation (24), (30), and (37), the internal relationship between elements with *SNR* of the Impossible Trinity are fully described.

When the second derivative equals zero, the *SNR* reaches its extremum, which represents the point where the growth efficiency of SNR is the highest or the lowest.

It is worth mentioning that the non-linear correlations among the other parameters of the model, excluding *C*, *D*, and *BER*, are also complex. Any change in one will result in significant changes in many affected parameters.

As shown in Fig. 4, there is a monotonous correspondence between the three elements. Each graph depicts the relationship between two key parameters, represented on the horizontal and vertical axes. The relationship is analyzed under the constraints of specific parameters such as B and P_r, serving as limiting factors.

C. User Demand Limitation and Performance Fluctuation

In real-world scenarios, communication demands higher performance across multiple aspects. For instance, in marine military surveillance, achieving a very low and stable *BER* is crucial to ensure the reliability of transmitted information.

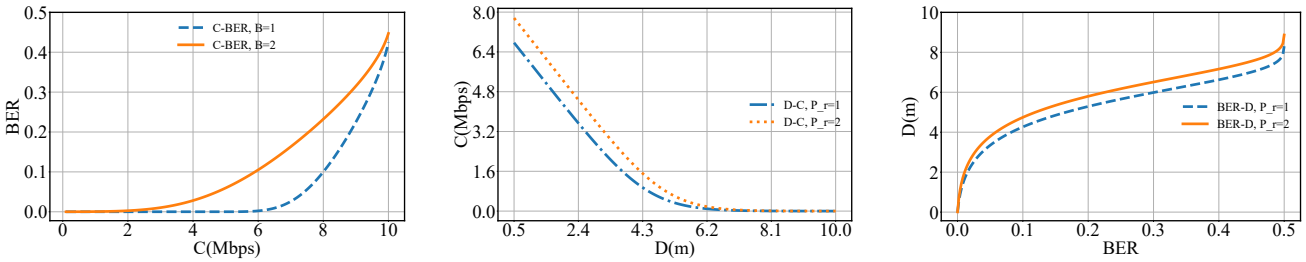

Fig. 4. Monotonous Correspondence between C, D, and *BER*

On the other hand, real-time applications in UOWC necessitate a higher maximum communication speed (C). These requirements create a complex landscape where the system must be optimized to meet users' specific demands. This optimization process involves drawing three quasi-fan shapes from the center point of the three performance elements.

As shown in Fig. 3, the three quasi-sectors which are constituted by the edges of the Impossible Trinity and the arc of user demand limitation narrow the acceptable range. The shadow part represents the acceptable range within the Impossible Trinity limited by user demand and variance.

Assuming that the constraints established by users regarding *BER*, C, and D are denoted as BER_{max}, C_{min}, and D_{min}, respectively, we can construe these minimum threshold values to be dictated by practical considerations.

In addition, the upper bounds are inherently dictated by a confluence of factors. The foremost among these are equipment and technological constraints which limit the potential enhancements in *BER*, C, and D. Meanwhile, considerations of energy costs add an additional dimension to this limitation, further shaping the maximal achievable thresholds.

The above models, however, are built for static environments. In practice, the elements are affected by the variance of the system device (i.e., σ_C, σ_D, and σ_{BER} correspondingly), and the dynamic interference of the channel (i.e., u_C, u_D, and u_{BER}). Subsequently, these constraints delineate the domain for the definition of the problem formulation, as:

$$\begin{aligned} C_{\text{min}} + \sigma_C + u_C \leq C \leq C_{\text{work}}, \\ D_{\text{min}} + \sigma_D + u_D \leq D \leq D_{\text{work}}, \\ BER_{\text{max}} - \sigma_{BER} - u_{BER} \geq BER \geq BER_{\text{work}}. \end{aligned} \tag{39}$$

Here, we clarify the intrinsic relationships and identify the key mutual constraints among the performance elements, providing essential insights for optimizing UOWC system performance to break through the first challenge. Subsequently, striking a balance between D, C, and *BER* becomes crucial when optimizing the performance of the system. Trade-offs need to be made to meet specific requirements and constraints, while considering the interdependencies among these factors.

D. Solver

In our work, we propose an optimization solver based on the Non-dominated Sorting Genetic Algorithm III (NSGA-III) [15], [16], [17], to tackle the UOCT Problem in UOWC in Algorithm 1. The devised NSGA-III-based solver begins by initializing a population with M random solutions. Each solution represents a feasible combination of D, *BER*, and C. Then, the fitness of each solution is evaluated, reflecting the overall communication performance under the trade-off.

Algorithm 1 NSGA-III based algorithm for UOCT problem

Input: population size N, iterations j, fitness function, parent population O_f.
Output: Non-dominated solutions sets O.

1: Initialize Population O_f with random solutions
2: Evaluate the fitness of each solution
3: **while** termination criteria not met **do**
4: Generate offspring O_s through crossover, mutation and tournament selection of O_f
5: Combine O_f and O_s to create a new population O_c
6: Perform fast non-dominated sort on O_c to generate fronts F_1, F_2, ..., F_n
7: Let O be an empty set and $i = 1$
8: **while** $|O \cup F_i| < M$ **do**
9: Add F_i to O
10: $i = i + 1$
11: **end while**
12: **if** $|O| \geq M$ **then**
13: Sort the solutions in F_i based on crowding distance in descending order
14: Add the first $M - |O|$ solutions from F_i to O
15: **end if**
16: **end while**
17: Return O as the set of non-dominated solutions

Algorithm 1 initializes a population O_f with M solutions, the objective function F, and a specified number of iterations j. Subsequently, the fitness of each solution is evaluated (lines 1-2). Then the iterative process begins, generating a new set of offspring solutions O_s through binary tournament selection, crossover, and mutation operations on O_f (lines 3-4). Afterwards, the algorithm merges the parent and offspring solutions, combining O_f and O_s to form a new solution set O_c (line 5). Thereafter, a fast non-dominated sorting operation is performed on O_c, segmenting the solutions into several fronts F_1, F_2, ..., F_n, based on their fitness (line 6). Then, selecting the next generation of solutions, an empty set O and an index $i = 1$ are initialized. The algorithm continuously adds fronts F_i to O until the size of O reaches or exceeds M. If so, the solutions in F_i are sorted in descending order based on their crowding distance, and only the first $M - |O|$ solutions from F_i are added to O (lines 7-14). Finally, the last step returns O as the set of non-dominated solutions after satisfying the number of iterations. It represents a set of optimal trade-off solutions for the UOCT Problem in the system (lines 15-17).

The NSGA-III-based solver navigates the multi-objective optimization landscape of the UOWC system. A Pareto-optimal solution set is identified, providing a range of optimal trade-offs for system design and operation.

E. Typical Solution Analysis

Within the solution set, special solutions exist. For instance, the corners of shaded area in Fig. 3 formed by the intersection of circular arcs denote the maximization of the elements to which they correspond. For example, the bottom corner of the shaded area indicates the maximum value of C. In a circular arc, the midpoint symbolizes the balance between two opposing elements, while minimizing the nearest one. For example, the circular arcs drawn from *BER* point mean the possible highest C and D while sacrificing the *BER* optimization in the acceptance range. The geometric center of the shaded area (i.e., acceptable range), equidistant from the three elements, underscores their equal importance.

These solutions carry specific meanings in practical applications. For example, in marine space intrusion detection, reliability takes precedence; in routine maritime environment monitoring, due to sufficiently long monitoring periods, erroneous information can be analytically ignored and there is low data volume requirements. Hence, maximizing D can reduce the number of nodes in a specific area for cost-saving, etc.

In terms of numerical performance, a single device under identical environmental conditions with different optimal strategies can achieve an 8-meter range with a *BER* of 10^{-6} and a communication speed of 1 Mbps, or a 4-meter range with a BER of 10^{-7} and a communication speed of 10 Mbps, satisfying the requirements of different environments.

In essence, this model and strategy can provide the highest performance strategy under specific scenarios and needs. This will enable users to formulate communication plans and select appropriate devices and strategies.

Based on complex relationships and resource constraints, we direct and optimize the expected performance elements with a feasible solution set to address the second challenge.

IV. Theoretical Analysis

In this section, we introduce the related theorems of the Impossible Trinity and present the corresponding proofs.

Lemma 1. *Given all other system parameters fixed, each SNR corresponds to a unique set of BER, C, and D.*

Proof. According to Equation (18), since the Q^{-1} function is continuous and monotonically decreasing in its domain (because Q^{-1} is the inverse function of the Gaussian error function, which increases monotonically in the real domain), Equation (18) is a continuous and monotonically decreasing function of *BER*. According to Equation (19), the exponential function and linear function are continuous, this function is a continuous function of C. Additionally, because the exponential function 2^x increases monotonically in its domain, this function is a monotonically increasing function of C. According to Equation (20), We find the partial derivative $\frac{\partial SNR}{\partial d}$ (see Equation (37)) and then analyze its sign due to the involvement of multiple parameters. For other parameters are fixed, since the $\mathrm{W}_0^{-1}(\cdot)$ function increases monotonically in its domain, Equation (20) should also increase monotonically with respect to D. Moreover, it can be easily found that *SNR* can be controlled in the range of *BER*, C, and D. As Equation (18), (19) and (20) are continuous and monotonic functions, and given that *SNR* is within the range of these three functions, we can infer that the system has unique solutions. ■

Lemma 1 is defined as a basis of the *UOWC Impossible Trinity*, according to Lemma 1, we describe the relationship between each of two elements and combine the three-dimensional diagram with the corresponding *SNR*.

However, in the complete system, the *SNR* can not be optimized in the real scenario. Lemma 1 provides a pre-optimization scheme for the system.

These three conditions are mutually exclusive in the given system. During the optimization process, the improvement of two or less out of low error rate, high communication rate, and longer communication distance inevitably leads to a decrease in one or more aspects. For example, increasing the D typically leads to a decrease in the average C or an increase in the probability of bit errors. Conversely, attempting to increase the average C while decreasing the *BER* would generally impose limitations on the achievable D. By analysing the properties of these elements, we can get the following theorem:

Theorem 1. *In a UOWC system, it is impossible to have all three of the following objectives at the same time inside the UOWC Impossible Trinity with fixed SNR:*

***Objective I**: Increasing communication distance D.*
***Objective II**: Increasing average communication speed C.*
***Objective III**: Steadily decreasing bit error rate BER.*

Proof. *In the premise of other parameters remain unchanged, there are three conditions and their opposite trends of the relationship among the BER, C, and D:*

- ***Increased** D **and** C **with limited BER**:* Assume we can achieve both increased D and increased average C from the *Objective I* and *Objective II*, while steadily decreasing *BER* from the *Objective III*. According to Equations (18) and (19), achieving the outcomes requires an increase in *SNR*. However, according to Equation (20), an increase in D leads to a decrease in *SNR*. According to Equation (18), a decrease in *SNR* results in an increase in *BER*, contradicting the initial assumption that we can increase D and average C without increasing *BER*.
- ***Increased** C **and Decreased BER with Limited** D:* Assume that we can achieve a higher average C and steadily decreased *BER* from the *Objective II* and *Objective III*, while increased D (*Objective I*). Both of these outcomes also require an increase in the *SNR*, according to Equations (18) and (19). However, if we could also increase D referring to Equation (20), this would lead to a decrease in the *SNR*, contradicting the need for an increased *SNR* to achieve the *Objective II* and *Objective*

III. Therefore, it is impossible to simultaneously improve the average C, decrease the *BER*, and increase the D.

- ***Increased*** D ***and Decreased BER with Limited*** C*:* Assume that we can achieve increased D and a steadily decreased *BER* from *Objective I* and *Objective III* while improving average C (*Objective II*). From Equation (18), reducing the *BER* requires an increase in the *SNR*. However, increasing D according to Equation (20) would decrease the *SNR*. The decreased *SNR* would then lead to a decrease in the C according to Equation (19), contradicting the initial assumption that we can extend D and reduce the *BER* without decreasing the C.

The contrapositive assumptions for the three conditions are proven invalid, thereby confirming the conclusion. ■

Theorem 2. *The UOCT Problem is NP-Hard.*

Proof. There is a correspondence between the elements of the UOCT Problem (*i.e.*, C, D, and *BER*) and the components of an Allocation Problem (the goods, agents, preferences), respectively. Moreover, connectivity constraints could analogously represent the constraints of the underwater communication environment. With such correspondence, UOCT Problem is a classic Pareto-Optimal Allocation Problem of Indivisible Goods with Connectivity Constraints [18]. Pareto-Optimal Allocation Problem is a classic NP-Hard Problem. Thus, the UOCT Problem is a NP-Hard Problem. ■

V. Simulation Analysis

We conducted extensive simulations to demonstrate the superior performance of our proposed model.

A. Simulation Settings

The simulation experiment for this work is designed with specific elements settings, enabling us to examine and evaluate the effects under various scenarios. The channel was set in an outdoor pool, a glass tank and a lake with different extinction coefficients: k = 20×10^{-4}, 40×10^{-4}, and 80×10^{-4} [19].

We set *SNR* to 10dB which are typical values for UOWC [20], [21]. The wavelength is set to 500nm as it is in a range between 475nm and 525nm [22] for blue and green light.

In terms of environmental factors, the temperature and pressure of the water were either ignored or set at typical values as 20 degrees Celsius and the pressure at 1 atmosphere, which are common conditions [22].

Through this simulation test, our aim is to provide a comprehensive understanding of the performance of both the Monte Carlo model [12] and traditional NSGA-III. This understanding will be enhanced by comparing their implementations of the Impossible Trinity model under various conditions.

B. Simulation Results and Analysis

This model excels in efficiently pruning the search. In our evaluations, *SNR* was fixed.

According to Fig. 5, given a specific *SNR* of 10, the optimization methods generate a solution set (C, D, BER) within a certain limited range. The results demonstrate the solutions identified in the corresponding timeframe. A traditional strategy, such as the Monte Carlo method [23] and NSGA-III would have to explore the entire feasible parameter space. In these simulation tests, our model introduces a more efficient search pruning method based on the Impossible Trinity principle, noted as NSGA Cut and MC Cut.

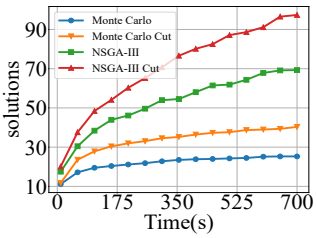

Fig. 5. Computational Efficiency

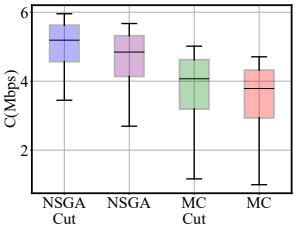

Fig. 6. Performance of C

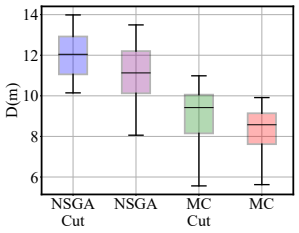

Fig. 7. Performance of D

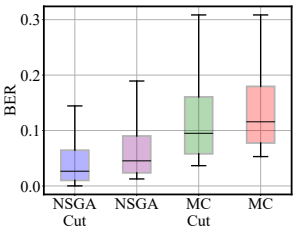

Fig. 8. Performance of *BER*

In this approach, the x-axis signifies time, while the y-axis represents the time required to find a solution that matches or exceeds a given threshold. This refined method promises significant search efficiency while preserving solution quality. Over the course of our analysis, we intermittently collected data points to track the optimal effects achievable by different methods within a given unit of time. This approach allowed us to simulate the optimization process and adjust the outcomes based on specific scenarios, thereby attaining performance metrics that align with user expectations.

Experimental evidence demonstrates that the NSGA-III with the Impossible Trinity model cut (i.e., UOCT) method has 28.57% more effective results than the sub-optimal method within the same computation time, on average.

In Fig. 6, Fig. 7, and Fig. 8, we contrast the performance of the traditional NSGA-III and Monte Carlo optimization methods with their enhancements incorporating the Impossible Trinity. Figures illustrate feasible regions for the vertical axes (C, D, *BER*) when other parameters remain constant. As can be discerned from the figures, our designed algorithm outperforms conventional optimization methods in three aspects: It achieves higher performance values, offers more precise value ranges, and has a median value closer to optimal performance. In these three aspects, NSGA-III with the Impossible Trinity surpasses the next best methods by margins of 14.43%, 21.27%, and 17.14%, for *C*, *D*, and *BER*, respectively.

VI. Test-Bed Experiments

To ascertain the validity of our model in practical applications in various UOWC systems, we conducted experiments in various scenarios (see Fig. 10) and under differing parameters using commercial off-the-shelf (COTS) equipment, comprising

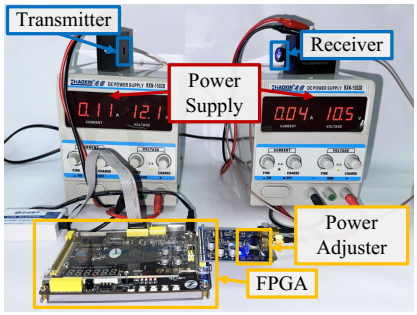

Fig. 9. Test-Bed Devices

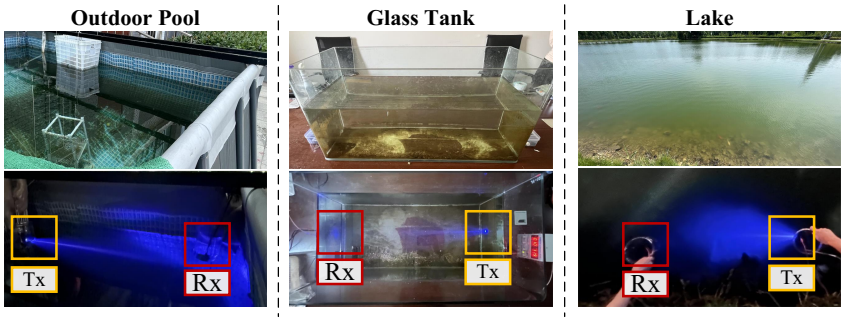

Fig. 10. Experiment Scenarios

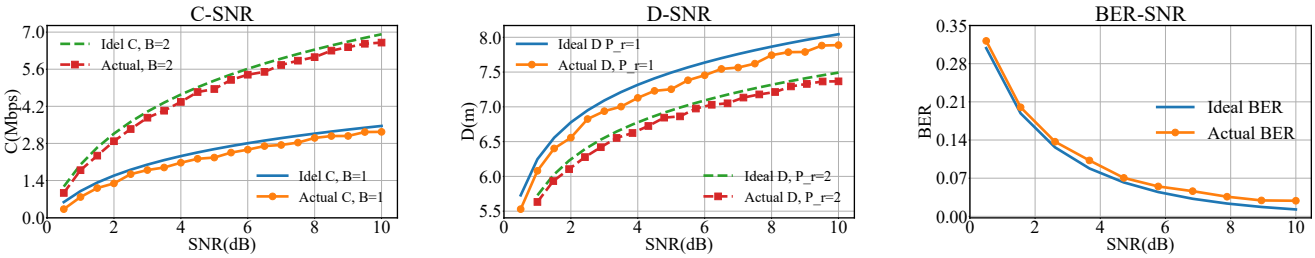

Fig. 11. Comparison of Theoretical Results and Experimental Results

an FPGA model, Cyclone IV ATK-DFEP4C, and an optical transceiver model, HCCL S2021MOD01, as depicted in Fig. 9. Note that visible light communication devices are capable of stable underwater communication and can also collect and relay information on their communication performance.

Our investigations were carried out in multiple environments: outdoor swimming pools, indoor glass tanks filled with turbid water, and natural lake water. Controlled experiments were performed at the transmitter end under specific electrical conditions, namely at 12V 0.1A, 6V 0.1A and 3V 0.1A. The aperture diameter of Rx is 1 cm, and the angle between Tx and Rx is controlled to be approximately 0 degrees. The communication distance can be adjusted within a range of 1 to 8 meters. Our methodology involved altering the angle of divergence of the emitted light beam, introducing interference, adjusting the optical efficacy, and optimizing the modulation scheme to increase C. We also incorporated forward error correction codes to enhance system robustness. The communication system was then tasked with complete data transmissions and compile metrics on its C, *BER*, and D performance characteristics.

TABLE I
PERFORMANCE IMPROVEMENT

Products	**OpenVLC**			**Shrimp**		
Elements	C	D	BER	C	D	BER
Performance Improved ↑	14.72%	19.66%	23.48%	22.39%	25.47%	20.13%

Furthermore, we selected two sets of commercial commodities (i.e., OpenVLC and Shrimp) [24], [5] for parameter optimization to enhance their performance. Experimental results demonstrated that, in our experimental environment, we filter the acceptance range by the optimal solution set of the Impossible Trinity, minimizing the mutual decrement of performance under limited resources. For a more intuitive effect, we optimized one performance at a time, aiming to minimally impact other performance, pushing performance elements closer to or into the acceptance solution range. We are pleased to find that the performance is improved by 20.48% and 22.66% on average. The performance improvements are illustrated in the Table I.

This improvement attributed to the resource waste caused by mutual constraints has been minimized, with resource allocation being optimized towards the expected aspects. Resources (e.g., power, bandwidth, processing capabilities) are wasted when the system attempts to improve a metric beyond the feasible limits set by the mutual constraints. For example, over-allocating power to extend communication distance might result in unnecessarily high power consumption without significant improvements in communication quality or reliability. Similarly, trying to minimize BER to very low levels might require excessive error correction, consuming more bandwidth and reducing overall communication efficiency. Based on experimental data, Shrimp outperforms OpenVLC slightly in the present experimental scenario. We attribute this superiority to the utilization of circular polarization and underwater bipolar coding scheme (UBC) in Shrimp [5].

The optimization enables the system to adapt to various application scenarios, thereby maximizing its utility. Given a fixed set of three performance elements, alternative parameter combinations may exist. For instance, two different systems might achieve the same C, D, and *BER* values with different transmitted power, divergence angle of the emitted light beam, and size of the receiver aperture. However, both systems can be effectively optimized using the Impossible Trinity model, introducing additional possibilities for system configuration.

As depicted in Fig. 11, we adjust a single parameter while

keeping others constant, then compare the trends of C, D, and *BER* as a function of *SNR*. We assess our model's accuracy by comparing empirical data with theoretical predictions.

To assess the accuracy of the model, we define the accuracy range. For *BER*, a deviation within an order of magnitude between predicted and actual values is considered acceptable. The acceptable deviation for *C* is identified as approximately 5 $Mbit/s$, based on demonstrated transmission rates in. For *D*, a 10% deviation is proposed as a standard [5].

TABLE II
ERROR OF THEORETICAL AND EXPERIMENTAL RESULTS

Elements	**D**		**C**		**BER**	
Parameter	$P_r = 1$	$P_r = 2$	$B = 1$	$B = 2$	$B = 1$	$B = 2$
Error	7.66%	4.29%	7.36%	8.56%	1.20%	0.74%

The experimental results validate that the predictive trend of the Impossible Trinity model is in perfect alignment with the theoretical predictions, with a maximum discrepancy between theory and reality not exceeding 8.56% and the average error remains at 4.85%. The error of theoretical and experimental results are shown in Table II.

Based on simulation analysis and test-bed experiments, the precision, feasibility, and superiority of the model performance optimization in *C*, *D*, and *BER* has been proved.

VII. RELATED WORK

In this section, we provide a comprehensive review of the literature on UOWC. We focus on three main aspects: performance parameters, optimization analysis, and model development and validation.

A. Performance Parameters in UOWC

Several researchers have contributed to improving and assessing UOWC performance parameters. For example, Yu *et al.* [25] conducted in-depth investigations into the fundamental factors that impact C and *BER* in various UOWC scenarios. Shlomi *et al.* [26] obtained the Meijer-G function for the end-to-end performance metrics of the SIMO-UVLC system. As a result, closed-form expressions for the system's Average Bit Error Rate (ABER) and outage probability were established. Nasir *et al.* [27] investigated the connectivity of Underwater Optical Wireless Sensor Networks (UOWSNs) and its impact on network positioning performance. They demonstrated that different network parameters, such as the number of nodes, the divergence angle, and transmission range, significantly affect network connectivity probability, highlighting the importance of transmission distance in their work. While the aforementioned works have made contributions to understanding certain aspects of UOWC system performance, few have explored the intrinsic relationships among multiple performance metrics and the constraints impacting overall performance.

B. Optimization Analysis in UOWC

To understanding individual parameters, recent research acknowledges the importance of considering trade-offs among these parameters. For instance, Saeed *et al.* [27] demonstrated that there exists a trade-off between *BER* and D in UOWC. This discovery challenges the traditional approach of optimizing individual performance parameters separately and stresses the necessity of combined optimization. Similarly, Huang *et al.* [28] highlighted the interaction between *SNR* and C, suggesting that a balance must be struck for optimal performance. However, these works only captured simple relationships and do not fully address the more realistic nonlinear multi-variable relationships which are closer to the real-world scenarios.

C. Model Development and Validation in UOWC

Model development plays a vital role in understanding and optimizing the performance of UOWC systems. For instance, models proposed by Emna *et al.* [29] addressed the statistics of optical beam irradiance fluctuations due to environmental factors in UOWC channels. Nasir *et al.* [30] modeled light noise sources and seawater channel impairments in UOWSNs. Ajay *et al.* [31] proposed a model that considers underwater channel degradation effects in UOWSNs. Existing models mostly focused on channel characteristics or specific aspects of UOWC systems or UOWSNs, with few offering a comprehensive consideration of the interplay among various factors.

Traditional methodologies often have a common issue: their exclusive focus on performance enhancement in specific aspects and overlook the potential losses associated with inherent limitations. In this work, we propose a comprehensive model that considers the trade-offs among performance elements, then facilitating the generation of feasible solution sets.

VIII. CONCLUSIONS

In this work, we introduce the "UOWC Impossible Trinity" model and theorems to enhance understanding and optimization of UOWC systems, successfully mapping key performance elements and inherent constraints. We propose the Underwater Optical Communication Trade-offs (UOCT) Problem, generating non-dominated solutions mindful of real-world restrictions and user demands, thus providing new pathways for optimization. Through rigorous simulations, our model, offering pragmatic system design and optimization guidelines, achieved over 95% practical accuracy compared to conventional models, while increasing communication distance by more than 20%. Our work pioneers solutions to UOWC optimization's intricate challenges, enriching knowledge of trade-offs and constraints in underwater communication.

In future work, we aim to expand the applicability of the model to guide not only other forms of underwater communication, but also optical communication in other environments, and even a broader range of applications.

IX. ACKNOWLEDGEMENT

We thank our anonymous reviewers for their valuable feedback. This research is sponsored in part by the National Natural Science Foundation of China under Grant 62172069.

REFERENCES

[1] Z. Zhao, C. Liu, W. Qu, and T. Yu, "An energy efficiency multi-level transmission strategy based on underwater multimodal communication in uwsns," in *IEEE INFOCOM*, 2020, pp. 1579–1587.

[2] C. J. Carver, Q. Shao, S. Lensgraf, A. Sniffen, M. Perroni-Scharf, H. Gallant, A. Q. Li, and X. Zhou, "Sunflower: Locating underwater robots from the air," in *ACM MobiSys*, 2022, pp. 14–27.

[3] K. Enhos, E. Demirors, D. Ünal, and T. Melodia, "Software-defined visible light networking for bi-directional wireless communication across the air-water interface," in *IEEE SECON*, 2021, pp. 1–9.

[4] C. J. Carver, T. Zhao, H. Zhang, K. M. Odame, A. Q. Li, and X. Zhou, "Amphilight: Direct air-water communication with laser light," in *USENIX NSDI*, 2020, pp. 373–388.

[5] C. Lin, Y. Yu, J. Xiong, Y. Zhang, L. Wang, G. Wu, and Z. Luo, "Shrimp: A robust underwater visible light communication system," in *ACM MobiCom*, 2021, pp. 134–146.

[6] J. Jang and F. Adib, "Underwater backscatter networking," in *ACM SIGCOMM*, J. Wu and W. Hall, Eds., 2019, pp. 187–199.

[7] M. Elamassie, F. Miramirkhani, and M. Uysal, "Performance characterization of underwater visible light communication," *IEEE Transactions on Communications*, vol. 67, no. 1, pp. 543–552, 2019.

[8] D. F. Swinehart, "The beer-lambert law," *Journal of Chemical Education*, vol. 39, no. 7, p. 333, 1962.

[9] E. P. M. C. Júnior, L. F. M. Vieira, and M. A. M. Vieira, "CAPTAIN: A data collection algorithm for underwater optical-acoustic sensor networks," *Computter Networks*, vol. 171, no. 107145, pp. 1–11, 2020.

[10] A. Goldsmith, *Wireless communications*. Cambridge University Press, 2005.

[11] N. Saeed, A. Celik, T. Y. Al-Naffouri, and M. Alouini, "Localization of energy harvesting empowered underwater optical wireless sensor networks," *IEEE Transactions on Wireless Communications*, vol. 18, no. 5, pp. 2652–2663, 2019.

[12] N. Saeed, T. Y. Al-Naffouri, and M. Alouini, "Outlier detection and optimal anchor placement for 3-D underwater optical wireless sensor network localization," *IEEE Transactions on Communications*, vol. 67, no. 1, pp. 611–622, 2019.

[13] F. Xiong, *Digital modulation techniques*. ARTECH HOUSE, 2006.

[14] D. J. MacKay, *Information theory, inference and learning algorithms*. Cambridge University Press, 2003.

[15] S. Mittal, D. K. Saxena, K. Deb, and E. D. Goodman, "Enhanced innovized progress operator for evolutionary multi- and many-objective optimization," *IEEE Transactions on Evolutionary Computation*, vol. 26, no. 5, pp. 961–975, 2022.

[16] K. Deb and H. Jain, "An evolutionary many-objective optimization algorithm using reference-point-based nondominated sorting approach, part i: Solving problems with box constraints," *IEEE Transactions on Evolutionary Computation*, vol. 18, no. 4, pp. 577–601, 2014.

[17] M. Geden and J. Andrews, "Fair and interpretable algorithmic hiring using evolutionary many objective optimization," in *AAAI*, 2021, pp. 14 795–14 803.

[18] A. Igarashi and D. Peters, "Pareto-optimal allocation of indivisible goods with connectivity constraints," in *AAAI*, 2019, pp. 2045–2052.

[19] K. Walcarius, J. Rosin, L. Hespel, M. Chami, and T. Dartigalongue, "Impact of blur on 3D laser imaging: Monte-carlo modelling for underwater applications," *Optics Express*, vol. 31, pp. 26 194–26 207, 2023.

[20] Y. Lou, J. Cheng, D. Nie, and G. Qiao, "Performance of vertical underwater wireless optical communications with cascaded layered modeling," *IEEE Transactions on Vehicular Technology*, vol. 71, no. 5, pp. 5651–5655, 2022.

[21] H. Lu, M. Jiang, and J. Cheng, "Deep learning aided robust joint channel classification, channel estimation, and signal detection for underwater optical communication," *IEEE Transactions on Communications*, vol. 69, no. 4, pp. 2290–2303, 2021.

[22] N. Chi, Y. Zhou, Y. Wei, and F. Hu, "Visible light communication in 6g: Advances, challenges, and prospects," *IEEE Vehicular Technology Magazine*, vol. 15, no. 4, pp. 93–102, 2020.

[23] M. Furqan Ali and D. N. K. Jayakody, "Simo-underwater visible light communication (UVLC) system," *Computer Networks*, vol. 232, no. 109750, pp. 1–11, 2023.

[24] A. Galisteo, D. Juara, and D. Giustiniano, "Research in visible light communication systems with openvlc1.3," in *IEEE WF-IoT*, 2019, pp. 539–544.

[25] M. Yu, C. T. Geldard, and W. O. Popoola, "Experimental comparison of modulation techniques for LED-based underwater optical wireless communications," in *IEEE WCNC*, 2023, pp. 1–6.

[26] S. Arnon and D. Kedar, "Non-line-of-sight underwater optical wireless communication network," *Journal of the Optical Society of America*, vol. 26, no. 3, pp. 530–539, 2009.

[27] N. Saeed, A. Celik, M. Alouini, and T. Y. Al-Naffouri, "Performance analysis of connectivity and localization in multi-hop underwater optical wireless sensor networks," *IEEE Transactions on Mobile Computing*, vol. 18, no. 11, pp. 2604–2615, 2019.

[28] J. Huang, Y. Lu, Z. Xiao, and X. Wang, "A novel distributed multi-slot TDMA-based MAC protocol for LED-based UOWC networks," *Journal of Network and Computer Applications*, vol. 218, no. 103703, pp. 1–12, 2023.

[29] E. Zedini, H. M. Oubei, A. Kammoun, M. Hamdi, B. S. Ooi, and M. Alouini, "Unified statistical channel model for turbulence-induced fading in underwater wireless optical communication systems," *IEEE Transactions on Communications*, vol. 67, no. 4, pp. 2893–2907, 2019.

[30] N. Saeed, A. Celik, T. Y. Al-Naffouri, and M.-S. Alouini, "Underwater optical sensor networks localization with limited connectivity," in *IEEE ICASSP*, 2018, pp. 3804–3808.

[31] A. Uppalapati, R. P. Naik, and P. Krishnan, "Analysis of M-QAM modulated underwater wireless optical communication system for reconfigurable uowsns employed in river meets ocean scenario," *IEEE Transactions on Vehicular Technology*, vol. 69, no. 12, pp. 15 244–15 252, 2020.